

# Electric resistance of a medium with a fractal structure

V. F. Gantmakher, S. E. Ésipov, and V. M. Teplinskiĭ

*Institute of Solid State Physics, USSR Academy of Sciences*

(Submitted 31 August 1989)

Zh. Eksp. Teor. Fiz. **97**, 373–383 (January 1990)

The changes of the electric-resistance curve  $R(T)$  produced in a metastable Zn–Sb alloy sample that is gradually annealed into an amorphous state has scaling properties. The residual ( $R_0$ ) and temperature dependent ( $R_1$ ) parts of the resistance are connected by the power law  $R_1 \propto (R_0)^{0.75}$ , while the dependence of  $R_1$  on  $T$  is described by a universal function in a wide range of  $R_0$ . A fractal branched model of the structure of the amorphous phase is constructed on the basis of the fact that the amorphization is accompanied by an increase of the specific volume. It is shown that the conductivity of an inhomogeneous sample containing a similar fractal system of insulating partitions can be reduced to the conductivity of a channel along the trajectory of a particle executing Brownian motion, i.e., along a diffusion trajectory. The foregoing relation between  $R_0$  and  $R_1(T)$  can be explained within the framework of this model with allowance for the classical size effect. The high-temperature deviations from the universal  $R_1(T)$  dependence are due to the finite conductivity of the amorphous phase.

## 1. INTRODUCTION

A metal–insulator transition accompanying a transition of a metastable metallic crystal phase of the alloy  $Zn_{0.4}Sn_{0.6}$  into an insulating amorphous state was observed in Ref. 1. The separation of the amorphous phase could be regulated by a stepwise annealing, in which the sample temperature was raised for a certain time to a value at which the sample resistance  $R$  began to increase noticeably with time. It was found that the amorphization is not uniform and leads during the intermediate stages of the process to a macroscopically inhomogeneous state. This follows from the fact that an increase of  $R$  by two or three orders of magnitude was not accompanied by a substantial shift of the temperature  $T_c$  of the superconducting transition; in a homogeneous state an increase of  $R$  would mean a decrease of the density of states of the carriers on the Fermi level, which would lead to a decrease of  $T_c$ . The assumption that the amorphous phase evolves from chaotically arranged spherical seeds does likewise not agree with experiment: the rather crude heat treatment used by the authors of Ref. 1 cannot alter smoothly and gradually the state of the sample in the immediate vicinity of the percolation threshold.

It was suggested in Ref. 1 that the amorphization takes place on the grain boundaries, i.e., on an initially specified fixed network of surfaces, and proceeds uniformly on all the boundaries. The assumption was that the resistance growth is due to an increase of the thicknesses of dielectric films. A painstaking examination of the dependences of the electric resistance on the metallic side of the transition, which are being discussed in the present paper, shows that the amorphous-phase layers are either not tied at all to the grain boundaries but are produced and grow independently, or else, while tied to the boundaries, do not produce on most boundaries the seeds of a geometrically more complex structure.

To clarify the formulation of the problem, imagine a sample in the form of an aggregate of grains of average dimension  $d$ . Its conductivity can be described by representing each grain as a lattice site and connecting neighboring sites by resistors. Prior to the start of the amorphization all the resistors are equal to  $\rho/d$ , where  $\rho$  is the resistivity of the

metal. This can be followed by two variants. If the boundary resistances become infinite randomly in succession, the conductivity of the medium is described by the equations of percolation theory. In this theory the resistance growth is due to the fact that the conducting channel between contacts becomes gradually longer and thinner, and the resistivity  $\rho$  of the conducting channel does not change. The total resistance  $R$  of a percolation cluster has therefore the simple temperature dependence

$$\frac{1}{R_0} \frac{\partial R}{\partial T} = \frac{1}{\rho_0} \frac{\partial \rho}{\partial T}. \quad (1)$$

Here  $R_0$  is the resistance of the sample and  $\rho_0$  is the residual resistivity of the substances making up the metallic cluster. The right-hand side of this equation does not change when the structure of the conducting channel changes during the amorphization, so that in the course of the latter

$$\frac{\partial R}{\partial T} \propto R_0^{-1}. \quad (2)$$

The second possibility is that the resistances of the boundaries increase gradually, being governed by the tunneling probability.<sup>1</sup> Recognizing that the tunneling resistance is independent of temperature, it is easily seen that amorphization should not influence the temperature-dependent part of  $\rho$ . We have therefore in the course of the amorphization

$$\frac{\partial R}{\partial T} = \text{const}, \quad \text{i.e.} \quad \frac{\partial R}{\partial T} \propto R_0^0. \quad (3)$$

Comparison of the changes of the temperature dependence with change of  $R_0$  can therefore cast light on the character of the structural changes that take place in the substance.

The foregoing considerations govern the content and plan of the present article. In the second section we analyze those results of Ref. 1 which pertain to the metallic side of the transition from the standpoint of the relation between  $\partial R/\partial T$  and  $R_0$ . This analysis leads to certain conclusions concerning the geometric characteristics of the conducting channels, which determine the conductivity during the ini-

tial stages of sample amorphization. The analysis is based on the assumption that both the geometric dimensions of the conducting channels and the residual resistivity depend on a parameter indicative of the degree of amorphization. This is possible if the parameter is the width of the conducting channels, and that the carriers in the channels are scattered mainly from their walls.

In the third section we justify our assumptions. Within the framework of elasticity theory, on the basis of the fact that the transition to the amorphous state is accompanied by an increase of the specific volume, we construct a branched (fractal) model of propagation of the amorphous phase. The presence of a fractal system of insulating surfaces leads to a specific structure of the conducting channels. Its analysis explains the experimentally observed power-law relation between  $\partial R / \partial T$  and  $R_0$ .

In the fourth section we demonstrate the presence of a correspondence between the conductivity of the conducting channel in this model and the conductivity of a conductor having the form of a diffusion trajectory. Using this analogy, we analyze the influence of the onset of conduction in the amorphous phase when the temperature is raised. The deductions of this analysis are also compared with experiment.

## 2. ANALYSIS OF THE DATA ON THE ELECTRIC RESISTANCE

### 2.1. Experimental results

We turn to the experimental  $R(T)$  curves<sup>1</sup> pertaining to the metallic side of a metal-insulator transition in the course of amorphization of a Zn-Sb alloy. The initial alloy sample is in a metastable state in a fine-crystalline metallic phase. It was obtained by cooling, to nitrogen temperature, a sample under pressure, followed by lifting the pressure. During each amorphization stage, following a stepwise anneal to a new state, the resistance  $R(T)$  was plotted in the temperature interval 4–100 K, in which heating does not yet alter the sample state.

Figure 1 shows the first seven curves of Ref. 1, plotted in

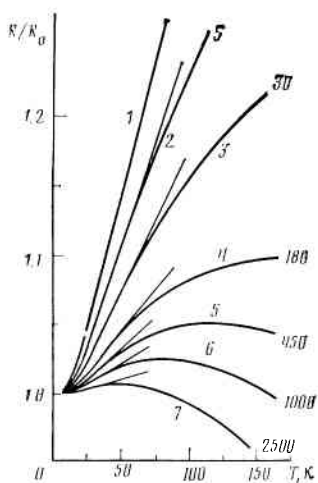


FIG. 1. Temperature dependences of the resistance of a sample during various amorphization stages. The curves are labeled, besides by the numbers 1–7, also by the ratio  $R_0/R_{01}$  of the residual resistance of the sample in the given state to its residual resistance in the initial state. Curve 1—temperature dependence in the initial state  $R_{01} = 0.61$  m $\Omega$ , corresponding to  $\rho \approx 50$   $\mu\Omega \cdot \text{cm}$  (Ref. 1).

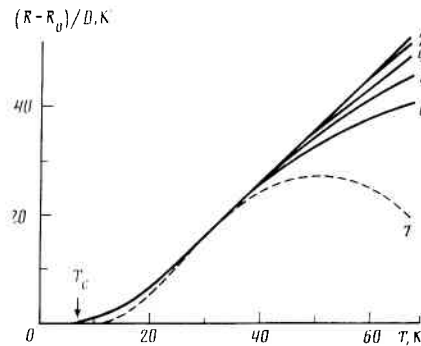


FIG. 2. The same as in Fig. 1, after renormalization to  $D = (\partial R / \partial T)_{T=30 \text{ K}}$ . Curve 7, which does not fit the universal dependence, is shown dashed.

a scale in which unity for each state of the sample is taken to be the resistance  $R_0$  at 7.1 K, above the superconducting transitions. All the curves have a temperature interval  $\Delta T \approx 20$  K in which  $R(T)$  varies linearly with accuracy not worse than 0.1%. Above this interval, the temperature growth slows down and the  $R(T)$  plot deviates from linearity. The deviation is earlier and faster the farther the amorphization has progressed.

Most important to us at present is that when  $R_0$  is increased the relative temperature increment of the resistance decreases even on the low-temperature part of the curve, where there is no deviation from linearity as yet. It has turned out that all the  $R(T)$  dependences in the temperature interval from 7.1 K to the value when deviation from linearity sets in are similar and can be superimposed by dividing by a corresponding scale factor (Fig. 2). We choose this factor to be the derivative on the linear section. The accuracy of the superposition is not worse than the random scatter of the points. The similarity begins to be violated when  $R_0$  increases by more than three orders, as demonstrated by curve 7 of Fig. 2.

Figure 3 shows a plot of the scale coefficient (the derivative on the linear section of the  $R(T)$  curves) against  $R_0$ . It can be seen that over a range of  $R_0$  exceeding three orders of magnitude we have the scaling-type power-law dependence

$$\frac{\partial R}{\partial T} \propto R_0^{0.75} \quad (4)$$

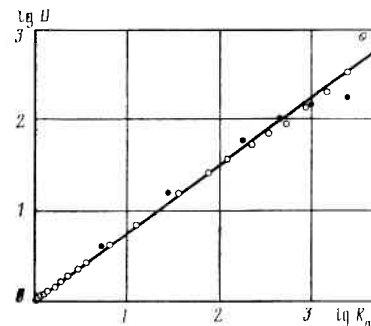


FIG. 3. Connection between  $D = (\partial R / \partial T)_{T=30 \text{ K}}$  and  $R_0$  for two different samples. Dark points—sample for which the measurement results are shown in Figs. 1 and 2. The straight line corresponds to an exponent  $\alpha = 0.75$  in Eq. (6).

Relation (4) is the principal experimental result subject to further discussion.

## 2.2. Geometric factor

As indicated in the Introduction, the amorphization process leads to an inhomogeneous state. We denote the characteristic dimension of the inhomogeneity by  $d$  and take it to be the parameter indicative of the degree of amorphization. We shall refine its physical meaning below, since the geometric structure can, generally speaking, be characterized by several lengths. For the time being, even the dimensionality of this parameter is immaterial.

We represent the sample resistance in the form

$$R(d, T) = R_0(d) + R_1(d, T) = R_0(d) + R_1(d)f(T) \\ = R_0(d) + R_1(d_1) [R_0(d)/R_0(d_1)]^\alpha f(T), \quad R_0(d) \equiv R(d, 0). \quad (5)$$

The first equality determines the subdivision of the resistance into residual and temperature-dependent, the second reflects the experimental universality of the dependence of  $R$  on  $T$ , and the third introduces a power-law relation between the terms  $R_0$  and  $R_1$  in the form

$$R_1(d) \propto [R_0(d)]^\alpha. \quad (6)$$

The value of the parameter  $d = d_1$  corresponds to the initial state of the sample (curves 1 in Figs. 1 and 2).

Relation (5) together with the value  $\alpha \approx 0.75$  contains all the discussed experimental data.

We express the sample resistance in the form

$$R = \rho \phi,$$

where  $\rho$  is the resistivity and  $\phi$  is a geometric factor. For a cylindrical conductor,  $\phi$  is the ratio of the sample length to its cross-section area. In our case  $\phi$  depends on the relative placement of the insulating amorphous layers, i.e., on the structure of the amorphous cluster. The factor  $\phi$  is common to  $R_0$  and  $R_1$ .

We represent the resistivity  $\rho(d, T)$  likewise by a sum of two terms

$$\rho(d, T) = \rho_0(d) + \rho_1(d, T), \quad \rho_0(d) \equiv \rho(d, 0). \quad (7)$$

Using (5) and (6), we obtain then  $\rho_1(d, T) = \rho_1(d)f(T)$ , where

$$\rho_1(d) \propto [\rho_0(d)]^\alpha [\phi(d)]^{\alpha-1}. \quad (8)$$

## 2.3. Size effect

The entire analysis that follows will be based on several assumptions.

1. The conductivity of the amorphous phase can be neglected, and its role reduces exclusively to formation of insulating partitions between the conducting channels.

2. The conducting metallic crystalline-phase channels exist all the way to the immediate vicinity of the transition of the sample into an insulator, with  $d$  the effective width of the channels.

3. The metallic channels are subject to a classical size effect due to carrier scattering by the channel walls.

The first assumption imposes an upper bound on the temperature interval in which the described model is valid. It appears that the conductivity of the amorphous phase cannot be neglected wherever the  $R_1(T)$  plot deviates from the

linear section of the universal  $f(T)$  curve. In other words, the interval is narrower the larger  $R_0$ . However, even on the curve 6 (Figs. 1 and 2) ( $R_0/R_{01} = 1000$ ) it extends all the way to  $T \approx 40$  K.

The second assumption will be discussed in Sec. 3. The third means that we neglect the mutual influence of the bulk and surface scattering processes. In the presence of such an influence the significance of the subdivision (7) itself is low, since the dependence of  $\rho_1$  on  $d$  can be quite complicated and the dependences on  $d$  and  $T$  may not factorize. For example, under weak-localization conditions changes of  $d$  can lead to a change of the effective dimensionality, and as a consequence to a change of the functional form of the  $\rho_1(T)$  temperature dependence. The assumption means therefore that  $\rho_0$  must not be too large, i.e., the model is not applicable in the immediate vicinity of a metal-insulator transition.

In the presence of a size effect,  $\rho$  can be expressed, accurate to several percent, in the form<sup>2</sup>

$$\rho(d, T) = \rho_0(d) + \rho_1(T) = \frac{p_F}{ne^2} \left( \frac{\beta}{d} + \frac{1}{l} \right), \quad (9)$$

where  $n$  is the carrier density,  $p_F$  is the Fermi moment,  $l(T)$  is the bulk mean free path, while  $\beta = 1$  for a wire and  $\beta = 0.4$  for a film. In the latter case  $d$  must not be too small:  $l/d < 10$ , since the  $\rho_0(d)$  dependence becomes logarithmic in the limit when  $d \ll l$ .

Substituting,  $\rho_0 \propto d^{-1}$  and  $\rho_1 \propto d^0$  in (8) we get

$$\phi(d) \propto d^\nu, \quad \nu = \frac{\alpha}{\alpha-1}. \quad (10)$$

The experimental value  $\alpha = 0.75$  yields

$$\phi(d) \propto d^{-3}. \quad (11)$$

It is instructive to compare the resultant  $\nu = -3$  with other cases. If a sample of volume  $L^3$  is converted into a coil of insulated wire with cross section  $s = d^2$ , its length is  $\lambda = L^3/d^2$  and  $\phi(d) = L^3 d^{-4}$ . This is the strongest possible power-law dependence of the function  $\phi$  on  $d$ . A tape of width  $L$  and thickness  $d$  has a length  $\lambda = L^2/d$  and hence  $\phi(d) = Ld^{-2}$ . Finally,  $\phi$  may not depend on  $d$  at all. For example, if an insulated wire of cross section  $s = d^2$  is cut into segments of length  $L$  and used to interconnect opposite side pairs of a cube  $L^3$ , with  $L^2/3d^2$  segments per pair of sides, we obtain a wattled cube with a factor  $\phi = 1/3L$ , i.e.,  $\phi \propto d^0$ .

## 3. KINEMATICS OF AMORPHIZATION PROCESS

### 3.1. Growth of amorphous phase

The experimental dependence (4) differs in principle from (2) and (3). This necessitates searches for another model of the structure of the sample's amorphous part. We start with the premise that a transition into the amorphous state is accompanied by an increase of volume.<sup>3</sup> It is clear even from the Le Chatelier principle that the transition has opposite reactions to the elastic stresses it produces—it is hindered in compressed regions and facilitated in the stretched ones. For an isotropic elastic medium it is natural to assume that a transition is possible when the strain causes the specific volume of some region to increase by a critical value  $u_0$ , i.e., if the trace of the strain tensor  $u_{ij}$  satisfies the condition

$$\sum u_{ii} - u_0 \geq 0. \quad (12)$$

A spherical seed cannot grow under such conditions, for the strains on its surface become negative before long. On the contrary, the planes growing a seed in the form of a flat disk compress the substance, but this leads on the edge to a tension that facilitates the phase transition. Naturally, the front of the amorphous phase moves with maximum velocity wherever it produces the largest tensile stress, i.e., where the left-hand side of (12) is a maximum. Without going into details of the complicated question of choosing the shape of the front, we confine ourselves to the statement that the moving front is similar to a blade that cuts into the metastable phase. The stability of the blade edge to breakup into needles is ensured by the fact that, other conditions being equal, the stresses on the edge of the blade exceed substantially those on a needle.<sup>4</sup>

We formulate now three rules that govern the front motion.

1. Weak planes (regions with small Young modulus) encountered in the path of a moving blade rotate the blade.
  2. The thickening of the blade behind the moving edge is very slow, since the medium surrounding it is compressed. The stress increases with time nonetheless, so that corners on the layer and inhomogeneously deformed regions serve as seeds for branching of the layers.
  3. The blade is stopped if it has to cross another blade.<sup>5</sup>
- In particular, if two blades converge at an angle, one of them will overtake and cause the other to turn away or stop, depending on the convergence angle. An exception is a head-on encounter.

We shall apply these rules, formulated on the basis of Refs. 4 and 5, to our problem. Layers of the dielectric amorphous phase propagate with practically no increase in thickness, become branched, and do not intersect. The latter is very important, since it means the presence of a mechanism that automatically prevents breaks of the conducting channel and subdivision of the sample into insulated granules. Instead, the conducting channel becomes branched in the course of the amorphization and becomes tortuous. The amorphous phase takes the form of "cacti"—trees with flat trunks and interlaced sprouts. Two-dimensional cuts through the structure during various stages of its formation are shown in Fig. 4.

### 3.2. Characteristic dimensions of structure

We introduce the concept of generations. Let the initial seeds have a density  $C$ . The surfaces that develop from them can have a characteristic area of order  $(C^{-1/3})^2$ . We call them the first generation, they form the trunks of the cacti. The second-generation sprouts have a characteristic dimension  $(2C)^{-1/3}$ , etc. The number of generations is determined by the shortest approach  $d$ , and its equal to

$$-3 \ln(C^n d) / \ln 2.$$

Amorphous sprouts are shown in Fig. 4 by thin lines. They have in fact a finite thickness  $\delta$  determined by the value of  $u_0$  and by the change of the specific volume in the transition; it should be obtained from the aforementioned problem of the front shape. It is probable that  $\delta$  depends on the generation of the sprout. The value of  $\delta$  determines the dielectric

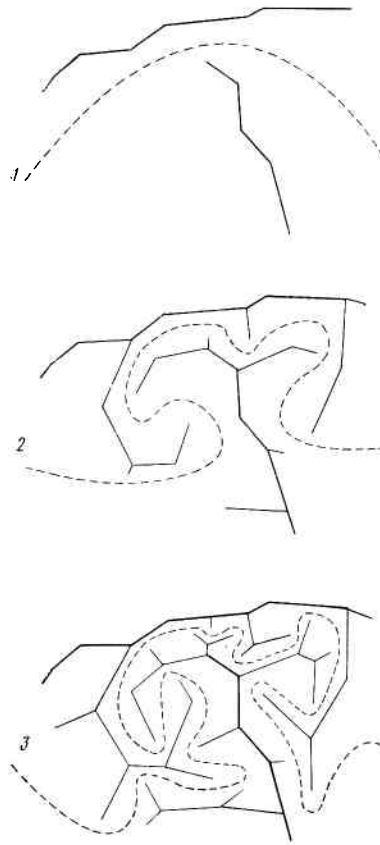


FIG. 4. Two-dimensional cuts of fractal structure of the amorphous phase during different stages (1–3) of its formation. Dashed line—trace of separating surface over which the conducting channels pass.

properties of the amorphous phase, for example the tunneling length.

This may not be the complete set of characteristic lengths of the structure. For example, there should exist one more scale—the branching length—which also depends on the generation. However, in view of the strong interaction via the elastic medium, all the scales cannot be assumed to be independent. By way of the simplest assumption we consider all the scales of the conducting channel to be of the same order. This is in fact the scale  $d$ . It is determined, as is also the number of generations in the structure, by temperature and time.

The length  $\delta$ , which does not enter directly in the description of the conducting channel, is an independent parameter. The foregoing arguments involving the concentration of the tensile stresses at the edge of a blade and the interaction of blades with one another are valid only if  $d \gg \delta$ . When  $d$  becomes comparable with  $\delta$  in the course of the amorphization, the stresses are equalized and coalescence of the amorphous layers should set in. At  $d \approx \delta$  approximately half the sample should be in the amorphous state. Recall in this connection that according to Ref. 1 the volume of the crystalline phase of Zn–Sb decreases by one-quarter at  $R/R_0 \approx 10^3$ .

An amorphous cactus is a typical fractal. This is easiest to verify by following one of the variants of the definition of fractal dimensionality in terms of the "capacity" of a set.<sup>6</sup> In this variant it is proposed to cover the investigated set with cubes of side  $\varepsilon$  and count the number  $K(\varepsilon)$  of these cubes; the dimensionality is then  $\ln K(\varepsilon) / \ln (1/\varepsilon)$ . A physical fractal

always has a range of scales  $\varepsilon$  in which it is defined; in other words, the dimensionality is approximately constant only in a certain interval of  $\varepsilon$ . In our case this interval extends from the distance between the initial germs of the amorphous phase to  $d$ , and  $d_{\min} = \delta$ . Since the distance between the cactus sprouts and the sprouts are present everywhere, to cover one cactus it is necessary to cover the entire volume for any  $\varepsilon > d$ . the dimensionality of an amorphous cactus is therefore equal to three.

### 3.3. Geometric factor of conducting channels

Let us break up the volume into regions that surround one germ each. Initially each boundary between two regions is a surface of dimension  $C^{-1/3}$  and of area  $C^{-2/3}$ . With growth of the amorphous phase, the boundaries of the regions containing individual cacti become strongly deformed. The deformed surface can be superimposed on one of the two cacti that separate it. This surface is therefore also three-dimensional.

Current should flow through a network of such surfaces. Since the surfaces are strongly cut-up, the lengths of the different paths between two points differ greatly. Therefore the current, tending to flow along a path with lowest resistance, i.e., the shortest path, tends to gather into ropes of current. They can also be called conducting channels. It is natural to assume their cross section area to be of order  $d^2$ . As the shortest line on a surface of dimensionality three, a conducting channel of length large compared with  $d$  has a dimensionality two. Over a size  $C^{-1/3}$  the length of such a channel is  $C^{-2/3}d^{-1}$ . Recognizing that for a cube with edge  $L$  we have a parallel connection of  $L^2C^{2/3}$  channels and that each channel has  $LC^{1/3}$  segments connected in series, we get

$$\phi = 1/LCd^3, \quad (13)$$

which coincides with the experimentally obtained dependence (11) of the factor  $\phi$  on  $d$ .

## 4. DIFFUSION TRAJECTORIES

### 4.1. Dimensionality of a conducting diffusion channel

The trajectory of a Brownian particle—a diffusion trajectory, is also two-dimensional in a three-dimensional space. In fact, consider a simple cubic lattice with dimension  $d$ . After  $N$  steps, the length of a diffusing-particle trajectory is  $Nd$ , and the average displacement of the particle from the start of the motion is  $N^{1/2}d$ . In other words, the trajectory increases as the square of the radius of that part of space which it occupies.

This raises the question whether current channels can be regarded as diffusion trajectories with steps equal to  $d$ . This calls for an estimate of the electric resistance of the diffusion trajectory with allowance for the self-intersections on it. The answer depends substantially on the dimensionality  $\zeta$  of the imbedding space. If  $\zeta = 1$ , the resistance is  $R \propto N^{1/2}d$ , but for  $\zeta \geq 4$  the opposite limit  $R = Nd$  is realized, since in a space of large dimensionality there are no self-intersections at all on a diffusion trajectory. In our case,  $\zeta = 3$ , we must estimate the contribution of loops and of more complicated configurations.

Let us show that the dimensionality of a diffusion trajectory in three-dimensional space remains unchanged if loops resulting from self-intersections are excluded. The tra-

jectory forms a ball contained in a sphere of radius  $N^{1/2}d$ . Through each of the  $N^{3/2}$  points inside this sphere can pass, with equal probability, a trajectory consisting of  $N$  steps. Consequently the passage probability is  $N^{-1/2}$ , and the probability of passing twice is  $N^{-1}$ . Therefore the number of points passed-through twice, i.e., the number of loops, is  $N^{3/2}N^{-1} = N^{1/2}$ . We estimate now the average loop length  $\bar{\lambda}$ . If  $p(M)$  is the probability of a particle returning to the initial point after  $M$  steps, then

$$\bar{\lambda}(N) = d \int_0^N dM M p(M) \propto \int dM M^{-1/2} \propto N^{1/2}. \quad (14)$$

Thus, a trajectory of length  $N$  has  $N^{1/2}$  loops that are on the average  $N^{1/2}$  steps long. Therefore, by cutting out all the loops, we change the length of the conducting channel by a value of the order of the initial length, and the remaining length is again of the same order. The geometric factor is therefore  $\phi(d) \propto d^{-3}$  as before. Although the remaining trajectory has no self-intersections, its length is by far not equal to the length, known in the literature, of the random-walk trajectory without self-intersections,<sup>7</sup> since the algorithms of their realization are entirely different.

In addition to isolated loops, a diffusion trajectory in three-dimensional space can contain more complicated configurations. For example, two loops can have a common section. Three parallel conducting paths connect corresponding two self-intersection points, so that all sections of both loops carry current. By reasoning as above we can show that allowance for such configurations likewise leaves the dimensionality of the conducting channel unchanged.

### 4.2. Shunting of loops

The deviations in Fig. 3 from a universal temperature dependence are due to the growth of the conductivity of the amorphous phase as the temperature is raised. We are dealing here not with tunneling but with thermoactivated conductivity. Let the resistivity of the amorphous phase be  $r(T)$ . Consider a plane central trunk of a cactus, with dimensions on the order of  $(C^{-1/3})^2$ . We break it up into squares of size  $d^2$  on both sides. The trajectory moves initially on one side of the plane trunk, and then on the other. The bending around the lateral sprouts is to us immaterial at present, since the corresponding sections of the trajectory are much shorter. The probability that a trunk section of size  $d^2$  will be passed-through by a trajectory from both sides can be easily calculated. It is equal to  $C^{2/3}d^2$ . Therefore the entire trunk contains only few (of order unity) such singular places where with rise of temperature the current will flow through the main trunk instead of along the trajectory. This shunting is more effective the longer the trajectory. Therefore, if the layer thickness  $\delta$  is the same on the entire cactus, the first to be shunted will be precisely the main trunks. This statement remains valid also if  $\delta$  depends on the number of the generation, but not very strongly.

We equate the resistances of the conducting channel and of the shunt:

$$r(T)\delta/d^2 = \rho(d, T)(C^{-1/3}d^{-1})/d^2.$$

Neglecting the dependence of  $\rho$  on  $T$  and putting  $\rho(d) \propto d$ , we get

$$r(T)d^2 = \text{const}. \quad (15)$$

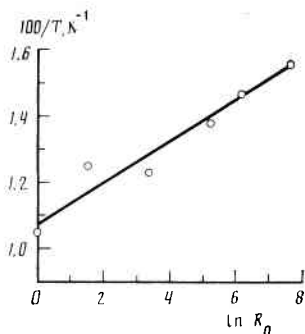


FIG. 5. Connection between the temperature at which the shunting action of the amorphous phase is manifested and the residual resistance  $R_0$ .

Assuming that  $r(T) \propto \exp(+A/T^\gamma)$ , we obtain

$$2 \ln d + A/T^\gamma = \text{const.},$$

or, using (9) and (10)

$$A/T^{\gamma-1/2} \ln R_0(d) = \text{const.} \quad (16)$$

Here  $\gamma$  can take on the value 1, 1/2, or 1/4, depending on the character of the conductivity of the amorphous phase (see, e.g., Ref. 8).

Figure 5 shows, as a function of  $\ln R_0$ , the reciprocal of the temperature at which the deviations from the universal temperature dependence reach 0.5%:

$$R_1(d, T) - R_1(d) f(T) \approx 0.005 R_0.$$

The scatter of the points is probably due to a certain leeway in the choice of the coefficients  $R_1$ . Notwithstanding this scatter, Fig. 5 can be regarded as a confirmation of Eq. (16).

Unfortunately, however, the accuracy is insufficient to determine and to clarify the conduction mechanism in the amorphous phase.

## 5. CONCLUSION

In the description of the conductivity of a two-phase material it is customarily assumed that the particles of both phases are randomly intermixed in an uncorrelated manner. This permits the use of percolation theory or of the effective-

medium theory. We have discussed in the present article the conductivity of an inhomogeneous sample with a structure of a different type, including a fractal insulating surface. This has led to the concept of the conductivity of a diffusion trajectory, which can apparently exist independently and have its own range of applications. We have succeeded in explaining, in the context of the formulated premises, the scaling character of the resistance curves  $R(T)$  in the discussed experiment at low temperatures, as well as deviations from it at high temperatures.

At the same time, the examination of the conductivity led to the problem of simulating the amorphization process or, in more general form, of a phase transition occurring in an isotropic solid and accompanied by an increase of the volume. A large number of the ensuing questions, concerning the form of the front, the interaction of the blades, the distribution of the dimensions  $d$ , the physical limit of branching, and others have only been named in this paper. They can undoubtedly be objects of further research, both theoretical and experimental. It is also important to search for new objects to which the concept developed in the present paper can be applied.

The authors thank V. V. Tvardovskii and D. E. Khmel'nitskii for helpful discussions, and O. I. Barkalov, I. T. Belash, and E. G. Ponyatovskii for interest in the work.

<sup>1</sup>O. I. Barkalov, I. T. Belash, V. F. Gantmakher, E. G. Ponyatovskii, and V. M. Teplinskii, *Pis'ma Zh. Eksp. Teor. Fiz.* **48**, 561 (1988) [JETP Lett. **48**, 609 (1988)].

<sup>2</sup>R. G. Chambers, *The Physics of Metals 1. Electrons*, J. M. Ziman, ed., Cambridge Univ. Press, 1969.

<sup>3</sup>I. T. Belash, V. F. Degtyareva, E. G. Ponyatovskii, and V. I. Rashchupkin, *Fiz. Tverd. Tela (Leningrad)* **29**, 1788 (1987) [Sov. Phys. Solid State **29**, 1028 (1987)].

<sup>4</sup>J. D. Eshelby, *Proc. Roy Soc. A* **241**, 376 (1957).

<sup>5</sup>J. Cook and J. E. Gordon, *ibid.* **A 282**, 508 (1964).

<sup>6</sup>J. Feder, *Fractals*, Plenum Press, 1988.

<sup>7</sup>P. de Gennes, *Scaling Concepts in Polymer Physics*, Cornell Univ. Press, 1979.

<sup>8</sup>B. I. Shklovskii and A. L. Efros, *Electronic Properties of Doped Semiconductors*, Springer, 1984.